



**HAL**  
open science

## Optimization of H2 thermal annealing process for the fabrication of ultra-low loss sub-micron silicon-on-insulator rib waveguides

Cyril Bellegarde, Erwine Pargon, Corrado Sciancalepore, Camille Petit-Etienne, Olivier Lemonnier, Karen Ribaud, Jean-Michel Hartmann, Philippe Lyan

► **To cite this version:**

Cyril Bellegarde, Erwine Pargon, Corrado Sciancalepore, Camille Petit-Etienne, Olivier Lemonnier, et al.. Optimization of H2 thermal annealing process for the fabrication of ultra-low loss sub-micron silicon-on-insulator rib waveguides. SPIE Opto 2018, 2018, San Francisco, United States. 10.1117/12.2289564 . hal-01942725

**HAL Id: hal-01942725**

<https://hal.univ-grenoble-alpes.fr/hal-01942725v1>

Submitted on 28 Feb 2024

**HAL** is a multi-disciplinary open access archive for the deposit and dissemination of scientific research documents, whether they are published or not. The documents may come from teaching and research institutions in France or abroad, or from public or private research centers.

L'archive ouverte pluridisciplinaire **HAL**, est destinée au dépôt et à la diffusion de documents scientifiques de niveau recherche, publiés ou non, émanant des établissements d'enseignement et de recherche français ou étrangers, des laboratoires publics ou privés.



Distributed under a Creative Commons Attribution 4.0 International License

# Optimization of H<sub>2</sub> thermal annealing process for the fabrication of ultra-low loss sub-micron silicon-on-insulator rib waveguides

Cyril Bellegarde<sup>a,b,c</sup>, Erwine Pargon<sup>a,b,c</sup>, Corrado Sciancalepore<sup>d</sup>, Camille Petit-Etienne<sup>a,b,c</sup>, Olivier Lemmonier<sup>d</sup>, Karen Ribaud<sup>d</sup>, Jean-Michel Hartmann<sup>d</sup>, Philippe Lyan<sup>d</sup>

<sup>a</sup>Univ. Grenoble Alpes, LTM, Grenoble, France, F-38042 ; <sup>b</sup>CNRS, LTM, Grenoble, France, F-38042; <sup>c</sup>CEA-Leti, Minatec, LTM, Grenoble, France, F-38054; <sup>d</sup>Univ. Grenoble Alpes, CEA-LETI, Minatec, F-38054

## ABSTRACT

The superior confinement of light provided by the high refractive index contrast in Si/SiO<sub>2</sub> waveguides allows the use of sub-micron photonic waveguides. However, when downscaling waveguides to sub-micron dimensions, propagation losses become dominated by sidewall roughness scattering. In a previous study, we have shown that hydrogen annealing after waveguide patterning yielded smooth silicon sidewalls. Our optimized silicon patterning process flow allowed us to reduce the sidewall roughness down to 0.25 nm (1 $\sigma$ ) while maintaining rectangular Strip waveguides. As a result, record low optical losses of less than 1 dB/cm were measured at telecom wavelengths for waveguides with dimensions larger than 350 nm. With Rib waveguides, losses are expected to be even lower. However, in this case the Si reflow during the H<sub>2</sub> anneal leads to the formation of a foot at the bottom of the structure and to a rounding of its top. A compromise is thus to be found between low losses and conservation of the rectangular shape of the Rib waveguide. This work proposes to investigate the impact of temperature and duration of the H<sub>2</sub> anneal on the Rib profile, sidewalls roughness and optical performances. The impact of a Si/SiO<sub>2</sub> interface is also studied. The introduction of H<sub>2</sub> thermal annealing allows to obtain very low losses of 0.5 dB/cm at 1310 nm wavelength for waveguide dimensions of 300-400 nm, but it comes along an increase of the pattern bottom width of 41%, with a final bottom width of 502 nm.

## 1- INTRODUCTION

The development of photonics mainly arises from Photonic integrated circuits (PIC) by exploiting compatibility with CMOS technology, notably through the use of silicon-on-insulator (SOI) circuitry [1]. Progress in the field led to PICs becoming more complex with a smaller footprint. Among the issues that come with size-reduction, the propagation loss of the circuit waveguides is a critical parameter that has to be assessed and minimized. Indeed, waveguides with sub-micron dimensions experience unacceptable optical losses, notably in the O-band (typically several dB/cm [2]). This is the case for the two structures typically used for wave guiding: Strip (rectangular-shaped) and Rib (Strip superimposed onto a slab). For both types of structure, the major part of the losses originate from waveguide's sidewall roughness, or Line-Edge Roughness (LER), which scatters light as the interaction between the optical mode and the sidewall imperfections becomes stronger with decreasing dimensions [3]. This difficulty can be tackled during the waveguide patterning process. Indeed, the main source of waveguide sidewalls roughness is the sidewalls roughness of the resist mask used to pattern the waveguide that is transferred into the stack during the plasma etching process. The first solution to reduce the silicon sidewalls roughness is then to introduce post-lithography smoothing treatment to reduce the photoresist (PR) roughness prior the etching [4]. The second solution is to introduce Si smoothing treatment after the waveguide patterning. The techniques commonly used include gas phase oxidation [5] and thermal annealing under H<sub>2</sub> ambient [6]. In a previous study, we demonstrated the beneficial impact of hydrogen annealing treatment applied after waveguide patterning to smooth the silicon waveguide patterns. Our optimized silicon patterning process flow allowed to reduce the sidewalls roughness down to 0.25 nm (1 $\sigma$ ) while maintaining rectangular Strip waveguides. As a result, record low optical losses of less than 1 dB/cm were measured at telecom wavelengths for waveguides with dimensions larger than 350 nm. [4].

In this work, we propose to investigate the impact of thermal annealing under H<sub>2</sub> ambient on the shape and roughness of Rib waveguides, and the consequence on their optical performances at a wavelength of 1310 nm. , We study the role of the presence of a Si/SiO<sub>2</sub> interface during the annealing by comparing the results obtained on Rib and Strip structures, as

well as by investigating the impact of the presence of a SiO<sub>2</sub> hard mask during the treatment. This work also shows the evolution of morphology and optical losses with annealing temperature and with annealing duration. This article shows that LER has been successfully decreased down to 0.7 nm by applying H<sub>2</sub> thermal annealing to Rib waveguide. Such a roughness reduction led to optical losses lower than 0.5 dB/cm at a wavelength of 1310 nm for waveguides wider than 350 nm.

## 2- EXPERIMENTAL SETUP

### 2.1. Substrates

Si/SiO<sub>2</sub> Strip or Rib waveguides were fabricated on 200-mm diameter SOI wafers with 310-nm-thick crystalline silicon layers on top of 800-nm-thick SiO<sub>2</sub> buried oxide (BOX), using a classical top-down approach. Wafers were patterned with 193-nm lithography in an ASML1100 stepper. A lithographic mask has been designed with lines having Critical Dimensions (CDs) ranging from 200 nm to 800 nm. The lithography stack coated on the SOI wafers comprised a 400-nm-thick 193 nm photoresist layer on top of an 82-nm-thick bottom antireflective coating (BARC) layer. When a hard mask was used, it consisted in a 100-nm-thick SiO<sub>2</sub> layer deposited prior to lithography.

### 2.2. Plasma etching tool and processes

Etching experiments were performed in a high-density plasma reactor generating an inductively coupled plasma (ICP). The waveguide patterning baseline process (BP) flow was slightly different depending on the masking strategy used. In the case of a resist mask, the photoresist patterns were exposed to a H<sub>2</sub> plasma treatment prior to BARC opening with an Ar/Cl<sub>2</sub>/O<sub>2</sub> plasma. Then Si was etched using an HBr/Cl<sub>2</sub>/He-O<sub>2</sub> plasma and the PR/BARC layers removed with an O<sub>2</sub> plasma. In the Hard Mask case, the photoresist patterns were transferred into the BARC layer with an Ar/Cl<sub>2</sub>/O<sub>2</sub> plasma then to the hard mask layer with a CF<sub>4</sub> plasma. After that, the resist/BARC layers were stripped with an O<sub>2</sub> plasma and Si etched using an HBr/Cl<sub>2</sub>/He-O<sub>2</sub> plasma. The Si etching depth was determined by the desired type of waveguide. For Strip waveguides, Si was etched down to the BOX whereas for Rib waveguides, only 150 nm of Si was etched. For both masking strategies, Si patterns were cleaned thanks to a dip in a HF 1% bath after patterning. In some cases, H<sub>2</sub> thermal annealing was introduced in the process flow at that stage. Once the waveguides were patterned with or without H<sub>2</sub> thermal annealing, a 100-nm SiO<sub>2</sub> hard mask was deposited and the wafers exposed to a second lithography step dedicated to the patterning of fiber grating couplers. After the etching of couplers, a 1.1- $\mu$ m-thick SiO<sub>2</sub> layer was deposited on the wafer to encapsulate the silicon waveguides. More details on the process flow can be found in reference [4].

### 2.3. H<sub>2</sub> thermal annealing

H<sub>2</sub> thermal annealing was used as a post-etching treatment to reduce the silicon waveguides sidewalls roughness. Such process induces surface atomic migration so that the surface energy is minimized [8]. The surface rearrangement leads to a surface roughness reduction and, if the thermal budget is too high, to a rounding of the sharp edges of the pattern. Those anneals are typically carried out in very high purity hydrogen in group-IV epitaxy chambers. The hydrogen flow is several tens of standard liters per minute. The hydrogen annealing process is controlled by the annealing temperature, chamber pressure, as well as its duration. In this work we studied the impact of temperature and annealing duration on the waveguide profile, roughness and optical performances. The influence of Si/SiO<sub>2</sub> interfaces has also been investigated.

### 2.4. Profile and Roughness characterization

After patterning, profiles of the silicon waveguides were characterized by scanning electron microscopy (SEM) cross-section observations.

Critical Dimension SEM (CD-SEM) is a common industrial technique to extract CDs and LERs of patterns from top-view SEM images. However, this technique shows some limitations when the pattern to be characterized presents a rounded and sloped profile, as it is sometimes the case for Rib patterns after annealing.

For this reason, we have used AFM measurements to characterize the sidewall roughness of our pattern. To that end, the sample was placed on a home-made sample holder that allowed the sample to be tilted so that the AFM tip could probe the pattern sidewalls. The measurement principle is shown in **Figure 1.a**. Because of the tilt, only one side of the pattern can be imaged. The patterns are scanned parallel to the lines. The tips used are 160AC-NA from Opus. AFM images are acquired in tapping mode. The free air amplitude is 2 V and the amplitude setpoint close to 1 V. The image size is rectangular (2  $\mu\text{m}$  along the x axis and 1  $\mu\text{m}$  along the z axis) and the scan rate of 0.5 Hz. For each image, 1024 lines of 1024 points were captured. After acquisition, AFM images were processed with a MATLAB script that rotates the image, interpolates points (**Figure 1.b**) and calculates the LER (which is equivalent to 3 times the root mean square (RMS) roughness) all along the pattern height (**Figure 1.c**). More details on the technique can be found in [9]. Fig. 1.b shows the reconstructed half-profile of a non-annealed Strip waveguide after patterning, and Fig. 1.c shows the results of Matlab computation, in terms of LER calculation along the pattern height. It is noticeable that the LER after Si patterning is constant along the pattern height and an average LER of 1.8 nm can be estimated. Therefore, we used this LER value as a reference for both Strip and Rib waveguides after patterning, as the only patterning difference between the two structures is the etching depth.

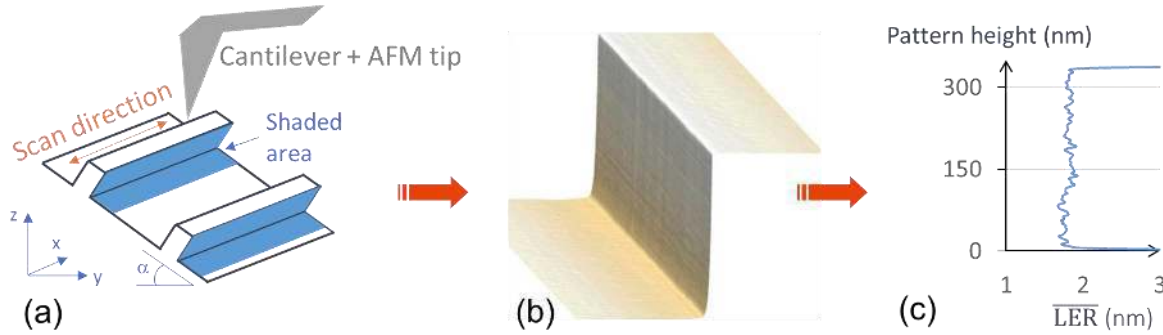


**Figure 1** (a) Schematic of AFM measurement on a tilted sample, allowing (b) half pattern profile reconstruction and (c) estimation of the LER along the pattern height and mean LER value.

## 2.5. Optical measurements

An on-wafer fiber probe system was used to characterize the propagation loss of the waveguides. A laser beam was coupled into and out of the structured waveguides via Transverse Electric-polarized grating couplers. A wavelength scan was performed in the 1260-1360 nm wavelength range to measure losses at 1310 nm. The power used was 1 mW, such that losses due to nonlinear effects were negligible. The transmitted power of the laser light through the waveguide was measured by a spectrum analyzer connected to the output fiber. Seven measurements were performed on waveguides with different lengths ranging from 2.2 mm up to 198 mm. When bends were necessary, the radius of curvature was 30  $\mu\text{m}$  such that bending losses were negligible at non-critical confinement factors. This set of measurements was repeated for seven waveguide's widths (ranging from 200 nm to 800 nm) on three dies of the wafer. The propagation loss reported in this work is the average of the measurements performed on each of the three dies over the wafer. Accuracy of the probe system is  $\pm 0.05$  dB/cm.

## 3- EXPERIMENTAL RESULTS

### 3.1. Impact of H<sub>2</sub> thermal annealing on Si waveguide profile and roughness

### 3.1.1. Role of the presence of Si/SiO<sub>2</sub> interface during the annealing

#### 3.1.1.1. H<sub>2</sub> thermal Annealing of Strip and Rib patterns

The impact of a Si/SiO<sub>2</sub> interface at the bottom of the pattern is investigated by comparing the impact of H<sub>2</sub> annealing on Strip and Rib waveguides. In the Strip case, the 310 nm Si layer is etched down to SiO<sub>2</sub> BOX. There is then a Si/SiO<sub>2</sub> interface exposed to the annealing process. In the Rib case, the etching process is stopped after etching half of the silicon layer thickness. In both cases the waveguides are patterned with a resist mask which is removed prior to the annealing.

The evolution of the Rib and Strip pattern profiles before and after H<sub>2</sub> annealing is shown in **Figure 2**. In the Strip case, the four corners are rounded, resulting in a swelled profile (Fig. 2.b) with convex corners. Top and bottom widths are reduced by about 50 nm, while the CD at mid height and the pattern height are preserved.

In the Rib case, top corners are rounded (convex corners) and a foot is formed at the bottom of the pattern (concave corners) leading to a tapered profile. Quantitatively, bottom width is increased by ~ 150 nm after annealing, while the pattern height remains constant.

Those differences show that a Si/SiO<sub>2</sub> interface at the bottom of the pattern locally limits Si reflow during annealing.

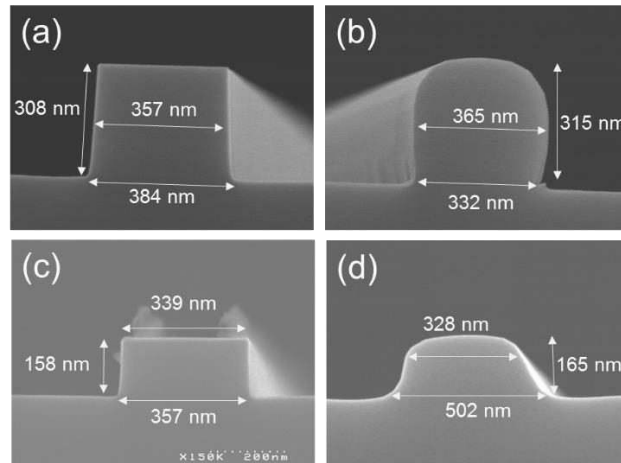


**Figure 2:** cross-sectional SEM images of (a) (b) Strip and (c) (d) Rib waveguides: (a) (c) without and (b) (d) with H<sub>2</sub> annealing. H<sub>2</sub> annealing conditions: 850°C, 20 Torr, and 2 min (resp. 1 min) for Strip (resp. Rib) waveguide.

AFM measurements on tilted samples were performed to evaluate the sidewalls roughness before and after annealing for both Strip and Rib waveguides. **Figure 3** shows the corresponding AFM profile and gives the average LER of the pattern sidewall. Before annealing, Rib and Strip waveguides have similar LER of 1.8nm (Strip profile provided in Fig. 3.a). Indeed, as shown in Fig 1.c, the LER is constant after etching along the pattern height regardless of the etched thickness. The roughness decreases for both Strip and Rib structures, but the improvement is greater in the Rib case (LER=0.7 nm only, corresponding to a 60% roughness decrease) than in the Strip case (LER=1.5 nm, corresponding to a 16% decrease).

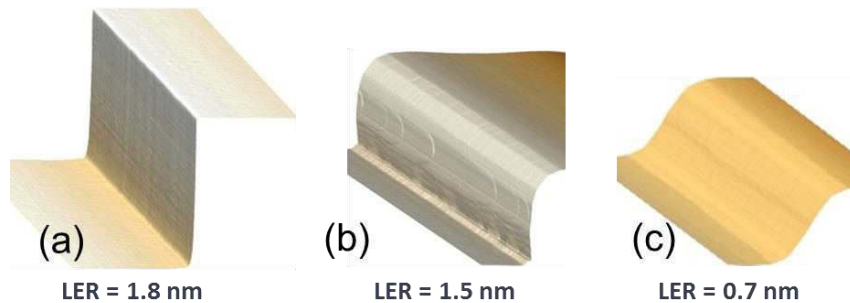


**Figure 3:** AFM profiles of (a) (b) Strip and (c) (d) Rib waveguides (b) (c) with and (a) (d) without H<sub>2</sub> annealing. H<sub>2</sub> annealing conditions: 850°C, 20 Torr, and 2 min (resp. 1 min) for Strip (resp. Rib) waveguide.

The presence of a Si/SiO<sub>2</sub> interface at the bottom of the pattern also limits the roughness reduction.

### 3.1.1.2. Presence of a SiO<sub>2</sub> hard mask during the H<sub>2</sub> annealing treatment

Rib waveguides are patterned using similar plasma etching conditions with either a photoresist or a SiO<sub>2</sub> hard mask. In the case of a PR mask, the resist is removed prior to H<sub>2</sub> thermal annealing. In the HM case, the SiO<sub>2</sub> is still in place during annealing. This allows us to evaluate the impact of a Si/SiO<sub>2</sub> interface at the top of the pattern during annealing. **Figure 4** shows cross-sectional SEM images of the Rib structure before and after H<sub>2</sub> annealing, this without (Fig 4.b) and with a SiO<sub>2</sub> HM (Fig 4.c) (Please note that, in Fig 4.c, the HM has been removed by a dip in HF after H<sub>2</sub> annealing for a better comparison between the pattern profile). In the latter case, the top corners are sharper with a HM than without, with a width difference of 60 nm at the very top of the pattern, indicating that Si reflow was locally less. Other dimensions such as height and bottom's width are similar for both masking strategies.

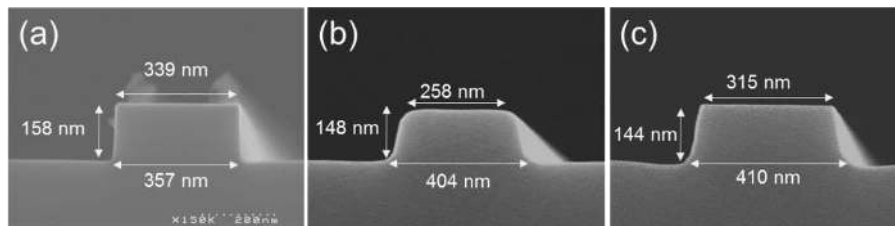


**Figure 4:** cross-sectional SEM images of Rib waveguides (a) before and (b) (c) after H<sub>2</sub> annealing; b) no mask is present during the thermal treatment, and c) a SiO<sub>2</sub> HM is present during the annealing and removed afterwards by a dip in HF for SEM observations. Patterns have been annealed at 850°C, 45 Torr, for 1 min.

Sidewalls roughness AFM measurements have been carried out before and after H<sub>2</sub> annealing for Rib patterned beforehand with PR (**Figure 5.a** and **5.b**) or a SiO<sub>2</sub> hard mask (Fig. **5.c** and **5.d**). Before annealing, the LER is lower if the waveguide is patterned with a resist instead of a hard mask (LER=1.8 nm vs LER= 2.4 nm). We have indeed shown in a previous paper that the hard mask opening step introduces some roughness increase [4]. After annealing, the roughness reduction is far more important without any hard mask in place during the annealing (45% roughness reduction vs 15% only with the presence of a SiO<sub>2</sub> hard mask). Those results once again confirm that the presence of a Si/SiO<sub>2</sub> interface limits the atomic surface migration and thus the sidewalls smoothening.

This preliminary study demonstrates the significant impact of a Si/SiO<sub>2</sub> interface in the mechanisms taking place during H<sub>2</sub> annealing. This interface limits the Si atoms diffusion on the surface, and consequently slows down the smoothening mechanism. On the other side, such interface locally favors the conservation of the waveguide shape.

The first consequence is that H<sub>2</sub> annealing conditions that are optimal for Strip waveguides in terms of pattern dimensions preservation and roughness reduction are not necessarily adapted to Rib waveguides that will be the subject of severe pattern reflow for the same annealing conditions. Secondly, in terms of sidewall roughness reduction, it seems more appropriate to pattern the Rib waveguide with a PR mask that is removed prior to annealing, this for two reasons. First, our baseline process (without the annealing treatment) is more performant in terms of LER if a PR mask is used (the use of a hard mask step results in some roughness increase). Second, the H<sub>2</sub> anneal is more efficient if there is no hard mask. Indeed, the sidewall roughness decrease is more important. Meanwhile, similar bottom dimensions increase (which could be detrimental to the Si circuitry design) occurs upon annealing with or without the presence of a hard mask.

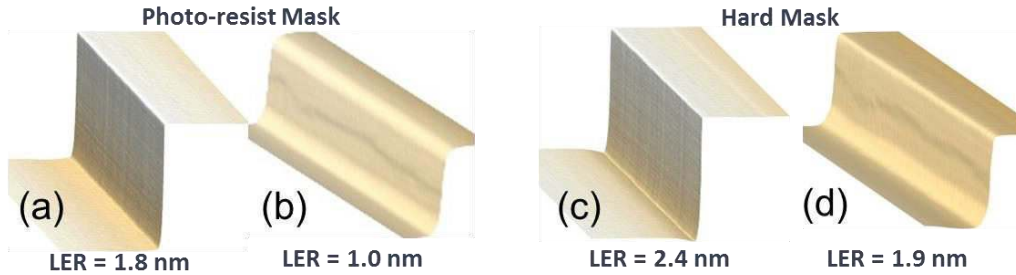


**Figure 5:** AFM profile and LER of Rib waveguides (a), (c) before and (b), (d) after H<sub>2</sub> annealing. The waveguides are patterned with (a), (b) a photoresist mask and (c), (d) a SiO<sub>2</sub> hard mask. The waveguides are annealed at 850°C, 45 Torr, for 1 min (b) without the presence of a mask, (d) with the presence of a SiO<sub>2</sub> hard mask. Note that the SiO<sub>2</sub> HM has been removed for (c) and (d) by a dip in HF prior to AFM measurements.

### 3.1.2. Role of Annealing Parameters

In this work we studied the impact of annealing parameters on the profile and sidewall’s roughness of a Rib structure patterned beforehand with a PR mask (removed prior to annealing). Several temperatures and annealing durations were tested.

#### 3.1.2.1. Annealing Temperature

The profile evolution with annealing temperature is shown in **Figure 6**. Pressure and annealing duration were kept at 20 Torr and 1 min. With increasing temperature patterns develop round top-corners and growing feet at the bottom. During annealing the bottom width increases by 17%, 41% and 92% when annealed at 800°C, 850°C and 900°C respectively. The waveguide height is maintained.

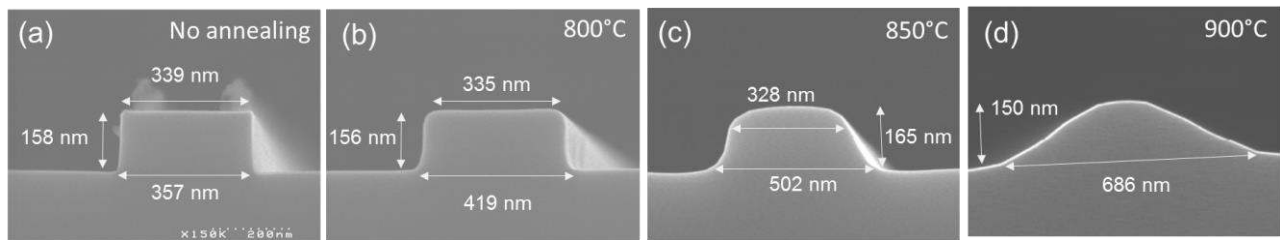


**Figure 6:** cross-sectional SEM images of a Rib waveguide patterned with a PR mask (removed after the patterning) as a function of the H<sub>2</sub> annealing temperature: (a) no annealing; (b) 800°C; (c) 850°C; (d) 900°C. Magnification for SEM images is 150k. Annealing pressure and duration are 20 Torr and 1 min., respectively.

The impact of annealing temperature on roughness is shown in **Figure 7**. AFM measurements were not performed for annealing at 900°C as the waveguide’s shape was not adapted for correct optical behavior. Average LER shows that the roughness decreases with increasing temperature as the Si reflow is more important. Compared to the baseline process, H<sub>2</sub> annealing at 800°C (resp. 850°C) reduces the LER by 39% (resp. 61%) down to 1.1 nm (resp. 0.7 nm).

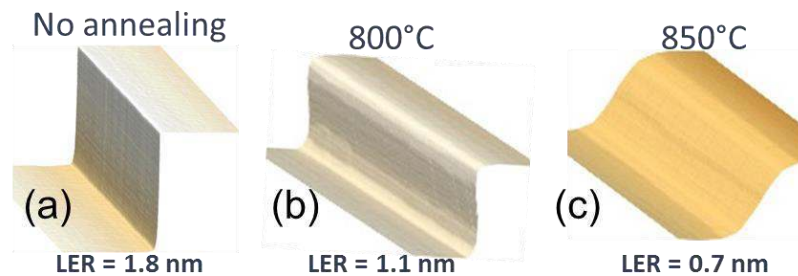


**Figure 7:** AFM profile of Rib waveguide (a) before and after H<sub>2</sub> annealing at (b) 800°C and (c) 850°C. Annealing pressure and duration are 20 Torr and 1 min., respectively.

### 3.1.2.2. Annealing duration

The second parameter investigated was the annealing duration. **Figure 8** shows the evolution of Rib waveguide profiles before and after 8 min. annealing at 800°C and 20 Torr. As expected, the waveguide top corners are rounded (the top width shrinks by 20%) and the bottom width increases (by 6%). The slight height difference of 6 nm between the two waveguides, is likely due to a slight difference in Si etching depth rather than an effect of the annealing treatment, as it was not observed in the other sections of this work.

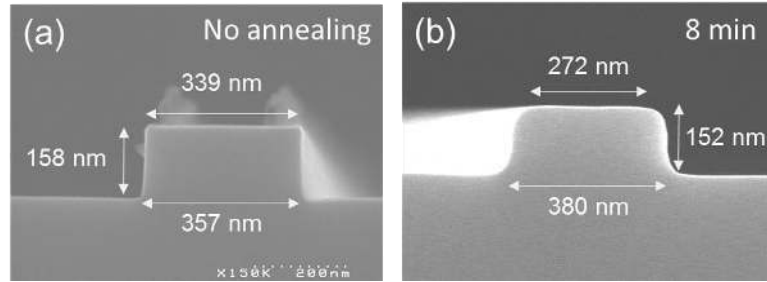


**Figure 8:** cross-sectional SEM images of rib waveguides (a) before and (b) after annealing during 8 min. Magnification for SEM images is 150k. Annealing temperature and pressure are 800°C and 20 Torr, respectively.

**Figure 9** presents the evolution of LER with annealing duration at 800°C and 20 Torr. After 1 min of annealing, the LER is reduced by 33% down to 1.2 nm. After 8 min, the LER decreased by 44% down to 1.0 nm. The roughness follows the expected behavior, i.e. the roughness reduction is enhanced as the annealing duration increases.

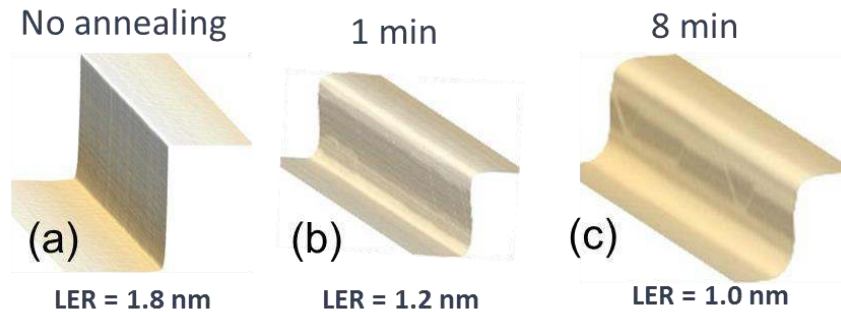


**Figure 9:** AFM profiles of Rib waveguide (a) before and after H<sub>2</sub> annealing for (b) 1 min and (c) 8 min. Annealing temperature and pressure are 800°C and 20 Torr, respectively.

## 3.2. Optical Results

In the previous sections, we have demonstrated the beneficial impact of H<sub>2</sub> anneals on Rib waveguide sidewalls roughness. The aim of this section is to quantify the beneficial impact on optical propagation losses of the significant roughness reduction induced by thermal annealing. The optical measurements are conducted at 1310 nm for waveguide width ranging from 300 to 800 nm.

### 3.2.1 Impact of the presence of SiO<sub>2</sub> hard mask during the annealing on optical losses

**Figure 10** shows the evolution of optical losses before and after annealing at 850°C and 45 Torr for Rib patterned with (i) a photoresist mask which is removed prior to annealing (Fig. 10.a) and (ii) with a SiO<sub>2</sub> hard mask still in place during annealing (Fig. 10.a). Let us first compare optical losses in Rib before annealing in Fig 10.a and 10.b. They are lower for



any CDs for the Rib patterned with a PR mask, consistently with the lower LER obtained (Fig. 5). In both cases, optical losses are significantly reduced after annealing. As expected, the loss reduction is better if there is no hard mask during the annealing (about 57% improvement in the PR case (Fig. 10.a) against 44% in the HM case (Fig. 10.b)). After annealing and in line with roughness measurements, losses are significantly lower when a PR mask is used beforehand, with a 40-50% improvement compared to the hard mask case. Thus the use of a hard mask appears as a severe limitation for optical performances at equal annealing conditions. Here, losses below 0.5 dB/cm are indeed achieved for CD>350 nm with a PR mask patterning, which is not reached with a hard mask patterning.

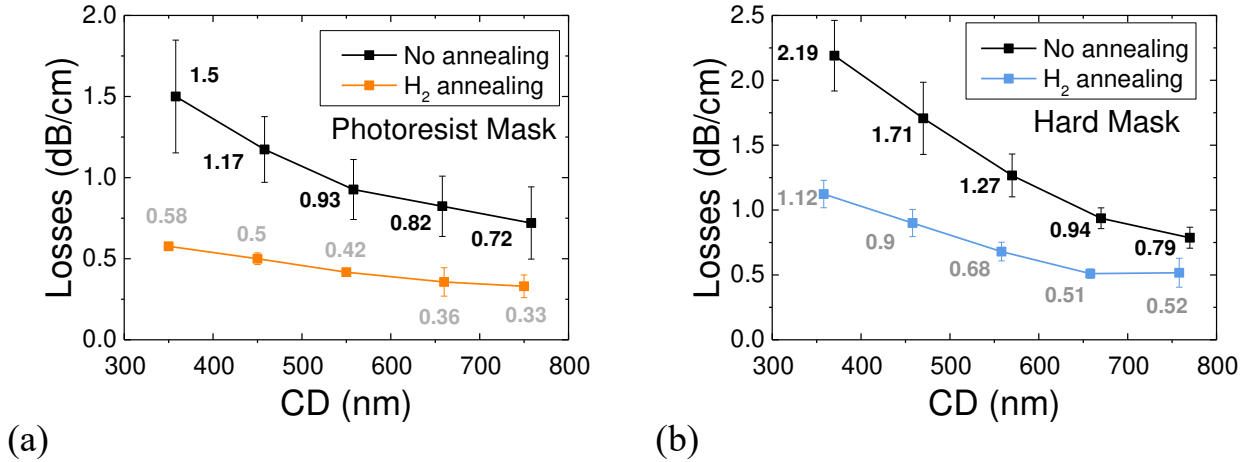


**Figure 10:** Propagation losses in Rib waveguide as a function of CD, when patterned (a) with a Photo-Resist mask or (b) with a hard mask (b), with and without H<sub>2</sub> annealing. H<sub>2</sub> annealing conditions: 850°C, 45 Torr, 1 min.

### 3.2.1.1. Impact of the annealing conditions on the optical losses

In this section, Rib waveguides were patterned with a PR mask which was removed prior to annealing.

### 3.2.1.2. Annealing temperature

The influence of annealing temperature on optical losses is shown in **Fig. 11**. Optical losses of Rib waveguides annealed at 800°C and 850°C (for 1 min. at 20 Torr) are compared to the baseline process performances. First, the effectiveness of the anneal is striking, with on average a 31% loss reduction for all waveguide CDs after annealing at 800°C, and 61% after annealing at 850°C. These percentages are equal to the roughness reduction percentages provided in section 3.1.2.1, which is surprising as the scattering losses typically scales with the square of the roughness [3]. For an annealing at 850°C, the optical losses are below 0.5 dB/cm for all CDs – starting at 350 nm - and go down to 0.29 dB/cm for the widest guide tested (CD=750 nm). From these results, it seems that the presence of a foot at the bottom of the Rib structures annealed at 850°C is not detrimental to optical propagation.

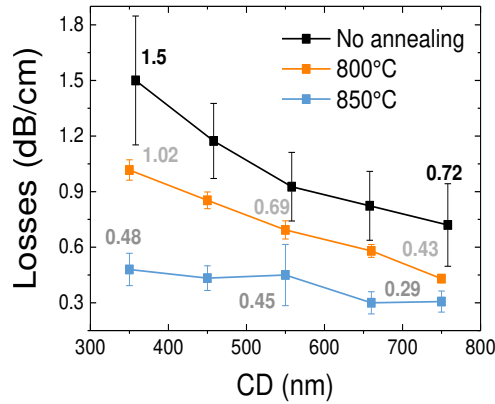


**Figure 11:** Propagation losses in Rib waveguide as a function of CD and annealing temperature. Other annealing parameters were 20 Torr and 1 min.

### 3.2.1.3. Annealing duration

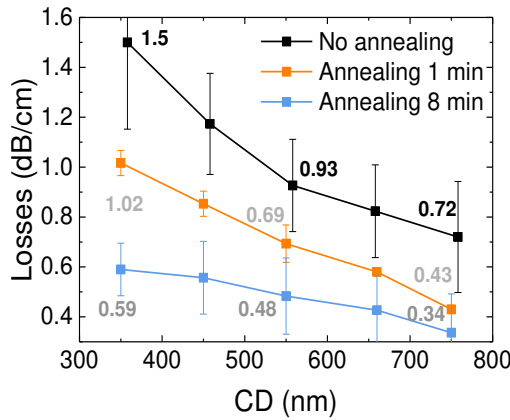


**Figure 12:** Propagation losses in Rib waveguide as a function of CD and annealing duration. Other annealing parameters: 800°C and 20 Torr.

The impact of annealing duration on optical losses is shown in **Figure 12**. Once again, the trend is fully consistent with the roughness reduction observed in Fig 9. Increasing annealing duration allows greater roughness reduction and consequently lower optical propagation losses; After 8 min annealing, an average 52% loss reduction is obtained for all CDs compared to the Rib patterning without any annealing, resulting in  $\sim 0.6$  dB/cm losses for CDs of 300-400nm.

## 4- CONCLUSIONS

Scattering losses in high index contrast Si/SiO<sub>2</sub> waveguides is known to be the primary cause of optical propagation losses. In a previous article, we demonstrated the remarkable benefit of using H<sub>2</sub> thermal annealing after Strip waveguide patterning in order to reduce the sidewalls roughness and consequently decrease optical losses. A record low optical loss of 1.3 dB/cm at 1310 nm wavelength was obtained for a Strip waveguide width of 350 nm annealed in H<sub>2</sub> at 850°C and 20 Torr during 2 min. The aim of the current article was to evaluate if the H<sub>2</sub> anneal could be transposed to the patterning of Rib waveguides. The main difference between a Rib and Strip pattern is the presence of a Si/SiO<sub>2</sub> interface at the bottom of the pattern in the case of Strip waveguides. This article shows that the presence of this interface has a key role in the mechanisms taking place during annealing: it limits the surface atomic migration and consequently slows down both the

Si pattern deformation and sidewall smoothening. Thus, although the optimal annealing conditions that were used for strip sidewalls roughness smoothening also result in significant decreases of the Rib LER, it leads to a severe increase of the bottom dimensions of the Rib waveguide, which may be detrimental for the design of the silicon circuitry. It should however be mentioned that the Rib height is not impacted by annealing. Similarly, we show that the presence of a SiO<sub>2</sub> hard mask during the H<sub>2</sub> annealing limits the beneficial impact of the post-etching anneal on roughness reduction. We then optimize the annealing conditions on Rib structures patterned with photoresist mask (removed prior to annealing) in order to find the best tradeoff between roughness reduction and pattern shape deformation. Decreasing the temperature to 800°C and increasing the duration up to 8 min seems a good compromise: it leads to a 44% roughness reduction and a 24% bottom dimension increase. Optical measurements performed on annealed Rib confirm that scattering loss has a dominant contribution to the total propagation loss, since the losses reduction scales with the roughness reduction induced by annealing. Optical data also reveal that the presence of a foot at the bottom of the rib pattern is not detrimental for mode propagation. The use of thermal annealing at 800°C and 20 Torr during 8 min allows to obtain very low losses of 0.6 dB/cm at 1310 nm wavelength for waveguide dimensions of 300-400 nm. Lower losses of 0.5 dB/cm can be obtained at higher temperature, to the detriment of bottom dimensions which increase. Ultimately, the optimal annealing conditions for Rib patterning depends on the final application: either ultra-low loss is desired no matter the waveguide dimension or the priority is given to dimension preservation.

## REFERENCES

- [1] Dumon P., et al., "Low-loss SOI photonic wires and ring resonators fabricated with deep UV lithography," IEEE Photon. Technol. Lett. 16(5), 1328-1330 (2004).
- [2] Horikawa T., et al., "Low-loss silicon wire waveguides for optical integrated circuits" MRS Commun 6(1), 9-15 (2016).
- [3] Payne F., Lacey J., "A theoretical analysis of scattering loss from planar optical waveguides," Opt. Quantum Electron 26, 977-986 (1994).
- [4] Bellegarde C., et al., "Improvement of sidewalls roughness of sub-micron silicon-on-insulator waveguides for low-loss on-chip links", Proc. SPIE 10108, 1010816 (2017).
- [5] Gao F., Wang Y., Cao G., Jia X., Zhang F., "Improvement of sidewall surface roughness in silicon-on-insulator rib waveguides," Appl. Phys. B 81(5), 691-694 (2005).
- [6] Gao F., Wang Y., Cao G., Jia X., Zhang F., "Reduction of sidewall roughness in silicon-on-insulator rib waveguides," Appl. Surf. Sci 252(14), 5071-5075 (2006).
- [7] Liao L., et al., "Optical transmission losses in polycrystalline silicon strip waveguides: effects of waveguide dimensions, thermal treatment, hydrogen passivation, and wavelength", Journal of electronic materials 29(12), 1380-1386 (2000).
- [8] Lee M. M-C, "Thermal Annealing in Hydrogen for 3-D Profile Transformation on Silicon-on-Insulator and Sidewall Roughness Reduction", Journal of Microelectromechanical Systems, vol. 15, no. 2 (2006).
- [9] Fouchier M., Pargon E., Bardet B., "An atomic force microscopy-based method for line edge roughness measurement", J. Appl. Phys. 113,104903 (2013)